Control Area

The Control Area soil profile consists of three horizons, distinguished in the field by color and texture (Table 1). The uppermost 1.5 cm constitutes an A horizon, having a pH of 5.98. This horizon shows relatively balanced properties of sand, silt, and clay, with characteristics of the clay size fraction accentuated more so than the other two particle size fractions. Between 1.5 and 14 cm, there is a change to a B horizon. The A to B horizon transition is also accompanied by a sharp increase in acidity to a pH of 4.16, and decreased in organic carbon content and LOI (Table 2). The decrease in sand content from CS1 to CS2 is an additional indicator of the transition out of an A horizon. Below 14 cm, there another B horizon marked by a color transition from [10YR 4/3] brown in the upper B horizon to [10YR 4/4] dark yellowish brown in the lower B horizon, accompanied by change in pH. This control area soil is similar to the profile within AOC 3, although it appears to be slightly less developed, with a somewhat truncated A horizon. Given the similarities between these two soils, including relatively low organic matter content within thin horizons indicative of an ochric epipedon, moderately acidic conditions, and location removed from any infill (Ball et al. 2004), this soil is an alfisol.

Area of Concern 7

The soil profile at AOC 7 (Fig. 3) includes four horizons, including two A horizons followed by two C horizons. Soil texture trends towards a decreased sand content and an increased silt content with depth. There is increasing alkalinity with depth, and high silica content associated with low overall organic C throughout. This soil has a high pebble content throughout the profile. The uppermost A horizon includes the top 5

cm of soil and has a pH value of 5.46. This horizon includes fine roots, small fragments of partially degraded organic matter, and pebbles. A decrease in observable organic matter particles and a slight decrease in pH marks the boundary from the uppermost A horizon to the second A horizon, which was determined to be from 5 to 11 cm. This transition is also accompanied by a clear texture change of increased clay content as well as a slight change in Munsell color.

From 7S1 to 7S2, there is also a steep decrease in organic carbon content and LOI, although there are low organic carbon levels found throughout the profile. Below the second A horizon, at a depth of 11 cm, there is an increase in silt content and decrease in sand content, which is indicative of a transition out of an A horizon. This horizon has a pH of 5.62. It is a distinctly different color from the A horizons above as well as the horizon below. The second C horizon is found at depths of 15 cm and below, and has a weakly acidic pH of 6.10. Rock fragments and pebbles are found in concentrations greater than or equal to surface horizon concentrations. The two horizons below the A horizons are interpreted as C horizons due to the slight texture and color changes, but otherwise there are no features that differentiate it from the rocky infill in the surrounding area. Due to the minimal horizon formation, this soil is classified an entisol.

Comparison of AOC 3, 7, and Control Area

Physical and chemical characterization of three profiles shows that there is greater similarity in elemental composition and chemical trends among soils from the control area and AOC 3 than between either of these soils and AOC 7, which is structurally and chemically quite different due to its different formational history and alteration. Variation

between AOC 3 and control area soils are due to differences in local topography, potential anthropogenic influence increasing topsoil erosion, and variations in the precise composition of parent material.

Figure 3. Pictures of soil profile at Area of Concern 7. Top of photograph is aligned with top of soil profile. Measuring tape for scale.

Control Area and AOC 3 show increasing acidity with depth, which is consistent with the Menfro soil series and associated soils found throughout Tyson Research Center (Ball et al. 2004).

Chemistry and Mineralogy

All soils have similar x-ray diffraction patterns (Fig. 4) that are dominated by quartz with a minor feldspar component. The similar mineralogy of these soils is typical of soil forming from silicate parent material. Further XRD measurements of the clay size fraction are needed to investigate possible variations in the mineralogy of the reactive fine fraction of the sediments.

The Control Area soil exhibits a distinct contrast between the organic carbon, LOI content, and SiO_2 concentrations between the top two horizons and the third horizon, which follows our interpretation of the transition out of an A into a B. There is also a decrease in the CaO content with depth. Other than these patterns and the minimal increase of Fe, Al, and Ti oxide content with depth, there are no substantial patterns among the major elements. Within the Control Area soil, there are minimally elevated concentrations of V, Cr, Co, Cu, Pb, and U in CS2, although, this soil exhibits far smaller ranges for all trace elements when compared to AOC 3 and AOC 7 because of lower concentrations overall. There are especially low Cu and Zn concentrations compared to AOC 3 and 7. Other than a decrease in Zn with depth, there are no other trends observed in the trace element composition of the control soil.

The profile at AOC 7 shows a weak trend in its decrease of organic carbon, TiO_2, Al_2O_3, MgO, and K_2O content with depth. However, none of these trends mark any

decreases of considerable magnitude, and overall, concentrations of major elements remain within a relatively small range. In terms of trace elements, AOC 7 shows higher Cr concentrations in the uppermost horizon, and high levels of Zn (97.2 ppm or greater) throughout the profile.

The AOC 3 soil profile has abrupt changes in the C_{org} and SiO_2 contents and LOI between the upper two horizons and the lower two horizons. There is roughly an 8% increase in SiO_2 content coupled to a 3.2% decrease in organic carbon at this transition point. The CaO content of the two upper horizons is approximately twice that of the two lower horizons. There are no chemical trends among the other oxide components. The lower 3 horizons of the AOC 3 profile align roughly with C_{org}, SiO_2, TiO_2 patterns observed throughout the three control area horizons, which follows the assertion that the control area is similar to the profile at AOC 3, with a truncated A horizon. Of the three soils, AOC 3 has the highest organic carbon and LOI content, which translates to the highest content of organic matter. In AOC 3, Cu, Zn, and Pb show similar trends with depth, with the highest concentrations of these elements in 3S2, comparable concentrations in 3S1 and 3S3, and the lowest concentrations in 3S4. Other trace metals in AOC 3 do not follow regular patterns. There are large errors associated with the total content of As, Se, and U, which limits the statistical significance of any observable trends of these elemental concentrations among the three profiles.

In terms of trace element composition, AOC 3 has considerably higher concentrations of Cu, Zn, and Pb than those of the control area, reaching levels of 139.3 ppm Cu, 286.9 ppm Zn, and 174.8 ppm Pb. These elevated concentrations are all found within the second A horizon, 3S2. Comparatively, this is nearly 11 times greater than the

control area's highest Cu content, roughly 5 times its highest Zn content, and about 5 times its highest Pb content. In comparison to AOC 7, these concentrations are just below two times its highest Cu content, just over two times its highest Zn content, and 2.6 times its highest Pb concentration.

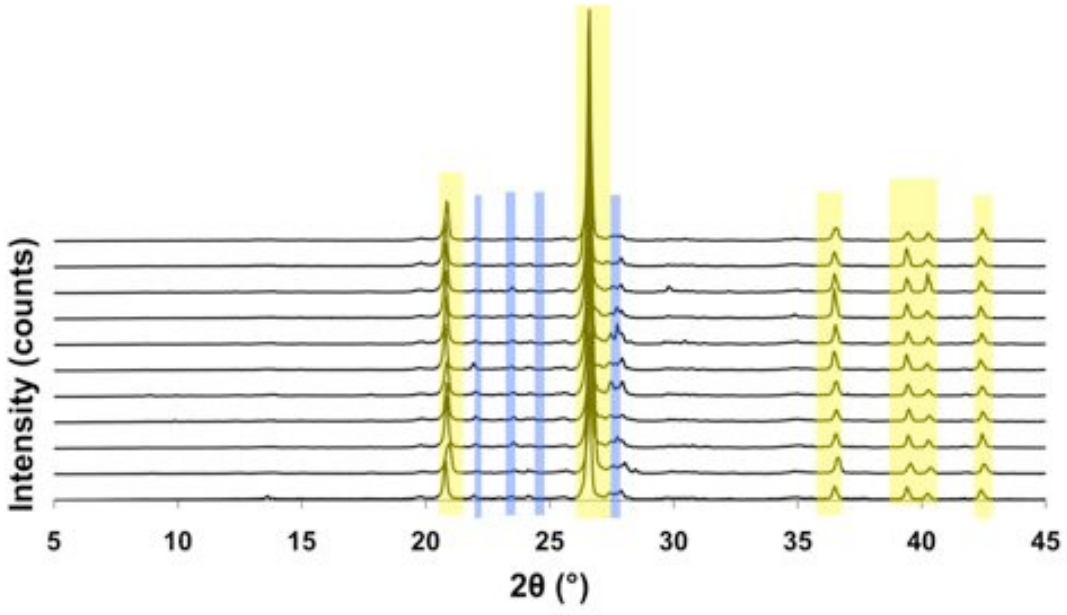

Figure 4. X-ray powder diffraction patterns of bulk soil (including sand, silt, and clay particle size fractions) from all sampling areas. Peak positions of dominant minerals shown by color: blue represents feldspar and yellow represents quartz.

Sequential Extractions

General Major Element Trends

The majority (roughly 60 to 98%) of the total concentrations of Mg, Al, Si, Fe, and K are not extractable, and remain in the residual fraction (Fig. 5). There are small fractions of these elements that are released during the extraction steps, exhibiting different behavior depending on species, but remaining mostly consistent across the three

soil profiles (Fig. 6). The low extractability of these major elements suggests that they are mostly found in weathering-resistant primary and secondary minerals.

Most Mg is found in the water soluble/exchangeable fraction, along with most Ca. There is a small portion of Mg that comes out in the upper horizons of all three soils during the organic matter step, as well as a similar amount extracted among all soil depths and all profiles in the reducible fraction. There is a consistent release of Ca during the acid soluble step; across all three soil profiles, Ca shows decreased release during this step with depth. Roughly equal amounts of Ca are extracted in the reducible fraction, although compared to total Ca values, these levels are very low. As discussed, the majority of K is not extractable. However, the fraction of K that is able to be extracted is released in three steps; some is released with Mg and Ca in the water soluble/exchangeable step, some is released during the reducible step, and a still sizable, although smaller fraction, is found in the organic matter step.

Of the extractable Fe (roughly 40% of total Fe), the majority is released in the reducible step (Fig. 6), which is expected given the redox nature of this element. In contrast to the substantial amount of Fe that is released during the extraction steps, more than 90% of Al remains in the residual fraction. Of the extractable Al, roughly half comes out during the organic matter step, ~20% in the acid soluble step, and ~30% in the reducible step.

Mn and P are extracted in much higher concentrations than the other major elements, with only roughly 10-30% of total concentrations remaining in the residual pool. The speciation of Mn is diverse, with fractions released in the three extraction steps. The majority, however, is extracted during the OM/MO step, as expected. P is mainly

extracted during the reducible step with a substantial fraction also released in the OM/MO step. Of all the major elements, Si is the least extractable, with concentrations ranging from roughly 320,000 ppm to just under 400,000 ppm remaining in the residual fraction. Extractable Si is released in roughly equal quantities during the organic matter and reducible extraction steps.

Major Element Trends by Soil

Ca exhibits similar trends with depth for AOC 3 and control area soils; it is released considerably more in the water soluble/exchangeable and acid soluble fractions towards upper horizons than in the lower horizons 3S3, 3S4, CS2, and CS3. The Ca released in these two fractions of the AOC 7 soil does not follow the same pattern. Small amounts of Ca are released evenly with depth and in relatively similar amounts across the three profiles during the reducible step, except for the absent fraction in CS1. Roughly even amounts are left in the residual fractions of all soils at all depths, likely as feldspar. The Ca released in the AS step is likely a result of acid attack on primary minerals, such as the feldspars common to these soils, while the Ca released during the reducible step is from the Ca associated with Fe. It is possible that this Ca is associated with Fe(III) clays that have the capacity to sequester Ca in the interlayers of the phyllosilicate sheets. Ca may also be released during this step from silicate minerals in which it is incorporated because of the removal of Fe oxide cements and exposure of silicate mineral surfaces.

Mg follows the same trend as Ca for the WS/EX step in terms of distribution among the three soils and with depth. Unlike Ca, however, no Mg comes out in the acid soluble extraction step, except for an anomalous portion in CS1. Mg is extracted in the

upper horizons of all three soils during the organic matter step, with none extracted in lower horizons. Roughly equal concentrations are extracted during the reducible step among all soils and depths, which may be a result of similar phyllosilicate sequestration as suggested for Ca extracted during the reducible step. In AOC 3 and Control area soils, there is more non-extractable Mg in upper horizons; this concentration decreases with depth. AOC 7 soil follows the inverse trend.

Unlike the similar patterns between AOC 3 and the control area for Ca and Mg, these two soils exhibit different behavior for K. Soil in AOC 3 has WS/EX and OM K concentrations that decrease with depth, while these reservoirs only release K in the top horizon for the control area, with no concentrations released in these pools at depth. CS1 also releases a small amount of K in the acid soluble fraction. K is not released from the acid soluble fraction in any other horizon across all soils. The amount of recalcitrant K increases with depth for all soils, located in primary mineral phases (e.g., potassium feldspar) or clays such as illite. The behavior of Ca, Mg, and K in the WS/EX fraction of the AOC 3 soil with depth (and the control area soil for Ca and Mg) is consistent with the pH-dependance of soil exchangeable cation composition.

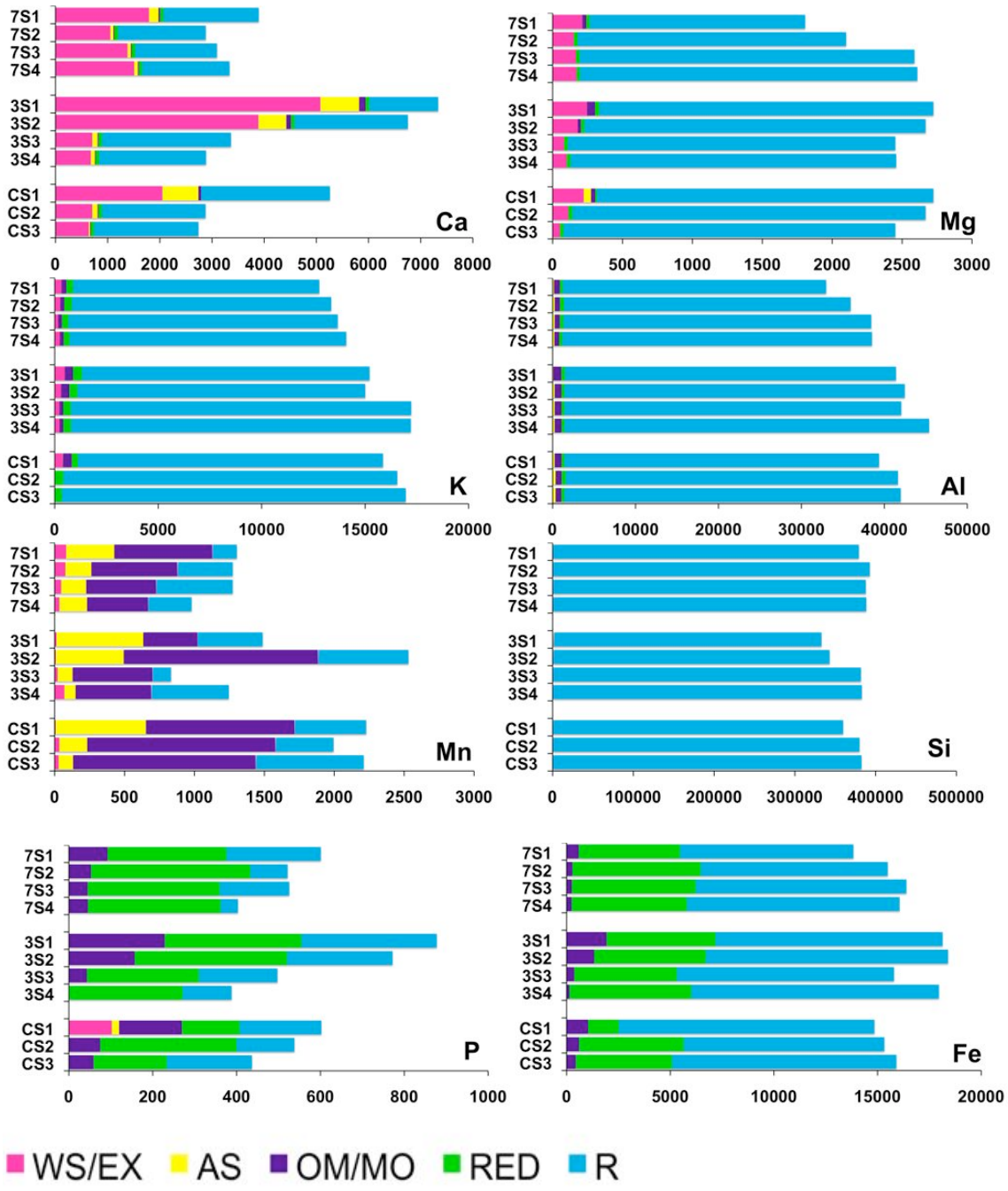

Figure 5. Major element release during sequential extractions. Concentrations (in ppm) shown on x-axis. (WS/EX: Water soluble/exchangeable fraction; AS: Acid Soluble fraction; OM: Organic Matter fraction; RED: Reducible fraction; R: Residual fraction. Plots arranged according to trends in distribution among elemental reservoirs.

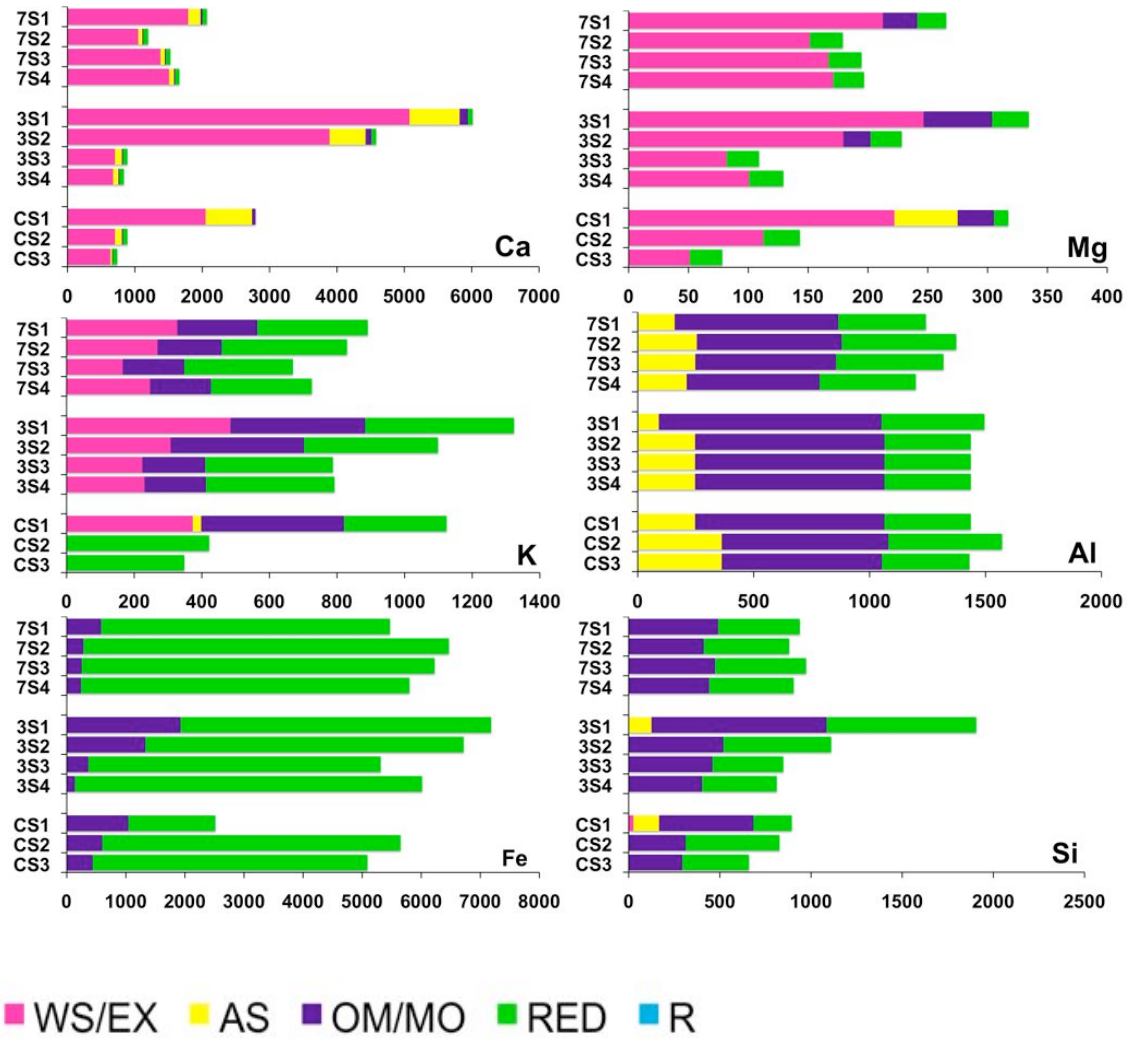

Figure 6. Major element release during sequential extractions shown without residual fraction (R). Concentrations (in ppm) shown on x-axis. (WS/EX: Water soluble/exchangeable fraction; AS: Acid Soluble fraction; OM: Organic Matter fraction; RED: Reducible fraction; R: Residual fraction. Plots arranged according to trends in distribution among elemental reservoirs.

The extractability of Al shows very little variation among the three soils or with depth within each soil, except that the amount released in the acid soluble fraction in surface horizons is only a fraction of the amount released in this fraction in deeper horizons; this pattern is similar across all soils. The Al released in the AS step could be due to partial dissolution of poorly crystalline aluminosilicates via acid attack. There is a large quantity of Al associated with the OM/MO fraction, as well as the RED fraction.

The release of Al during the OM/MO step is likely due to Al being extracted from Al-humic acid or Al-humate-mineral complexes (Violante et al. 1999). The Al released during the RED step is likely Al incorporated into Fe oxides (Cornell & Schwertmann 2003). This data cannot conclusively determine whether Al is most strongly associated with Fe-oxides, Mn-oxides, or organic matter.

Fe shows similar behavior across the three soils, but is best aligned in terms of speciation between AOC 3 and the control area. Much of the extractable Fe is released during the reducible step, consistent with the redox chemistry of this element. Fe comes out in greater concentrations in the organic matter fraction towards the top of each profile, with decreasing amounts extracted in this step with depth; this fraction is likely due to the presence of Fe-humic complexes. The pattern of Fe extracted during the reducible step follows the opposite trend, because of Fe released from poorly crystalline Fe oxides (Shang & Zelazny 2008). Concentrations of extractable Fe are fairly constant with depth, which suggests that Fe speciation is depth-dependant due to the different amounts of organic matter and Fe oxides that change along the profile.

The extractable Si follows very similar patterns between the soils of AOC 3 and the control area. It is released in small amounts in the top horizons of both of these soils during the acid soluble step, then is extracted in decreasing concentrations in the organic matter and reducible steps with depth. Si comes out in relatively even amounts in all horizons of AOC 7. Anomalously, a very small amount of Si is extracted in the WS/EX step in CS1. However, the vast majority of Si (>98%) is in a recalcitrant phase, which is expected given the resistance of quartz and feldspar to weathering and their slow dissolution kinetics under the conditions of the extraction fluids (Brantley et al. 2008).

P is released during the OM/MO step in decreasing amounts with increasing depth for all three soils. There is no P extracted in this step in the bottommost horizon in AOC 3. Some P is extracted during the water soluble/exchangeable and acid soluble steps in CS1, although this is an outlier among the other P release patterns. A substantial fraction of P is also removed during the reducible step. P follows trends that are very similar to those seen in the Fe extractions, which suggests there may be a close association of P with Fe-oxides, likely as adsorbants on surface sites of Fe oxides (Cornell & Scwertmann 2003).

Extracted Mn in the WS/EX and AS phases follows similar patterns for AOC 3 and Control Area soils, showing minimal WS/EX release in the A horizons with increased release in the B horizons, and the opposite trend for the AS fraction. WS/EX Mn follows the inverse pattern for AOC 7, with a weak trend towards lower concentrations with depth in the AS fraction. The WS/EX Mn is likely exchangeable Mn^{2+} (Pendias & Kabata-Pendias 2000). Mn may be extracted during the AS step because of acid attack on Mn-oxides. As expected, a substantial fraction of total Mn is extracted during the OM/MO step. No Mn comes out during the RED step with Fe-oxides, likely due to the remainder of extractable Mn coming out in the OM/MO step. There is also residual Mn, potentially in a silicate phase.

Trace Element Trends

Of the nine trace elements under investigation, Cr, As, and Zn were generally not extractable (Fig. 7), although Zn shows some inconsistent behavior in the top horizons of AOC 7 and the control area. Overall, though, the bulk of these elements remain in the

residual reservoir, which means they are largely immobile. The low extractability of Cr is consistent with the expected solubility of Cr(III) (Rai et al. 2004; Rai et al. 2002).

Extractable V, which is roughly 20% of total V, comes out in the reducible step, showing an association with Fe-oxides. It is possible that V was incorporated into the structure of goethite or hematite as V(III) (Schwertmann & Pfab 1996; Cornell & Schwertmann 2003); phase analysis by spectroscopic methods could provide more information on the speciation of this element. Pb shows similar behavior to V with its main reservoirs being the reducible fraction and the residual fraction, although this element is generally extracted in higher concentrations during this step than V, and there is much less left in the residual fraction. Pb extracted from the reducible fraction suggests a strong association with Fe-oxides, possibly in an adsorbed or incorporated form (Bradl 2004).

Cu and Ni exhibit similar associations, with the main extractable content releasing during the organic matter step. In comparing the quantities of these two elements released, Ni is extracted in substantially smaller concentrations during this step, with a greater percentage remaining in the residual fraction (Fig. 4). Cu often forms inner-sphere complexes with humic substances (Bradl 2004; Yin et al. 2002), and is preferentially captured by organic matter in comparison to Ni. These two elements are also strongly associated with Mn-oxides (Quantin et al. 2008; Vega et al. 2006).

Co and Se also show parallel trends, with substantial portions extracted in both the OM/MO and RED steps, and nothing left in the residual fraction. Co is strongly adsorbed and incorporated into Mn-oxides (Burns 1976) as well as Fe oxides (Bradl 2004) while Se is commonly bound to the surface of organic matter and Fe or Mn-oxides

(Seby et al. 1997). Total extractable Co and Se exceed their bulk contents determined by XRF and the residual components of these elements were thus unconstrained. We infer that Co concentrations determined by XRF may be systematically and consistently low due to fluorescent lines for this element occurring near fluorescent lines for the major element Fe. The disparity between Co concentrations extracted and total Co determined by XRF is on the order of 20 ppm. In contrast, there is an enormous difference in the Se extracted and the amount detected by XRF, on the order of 80-100 ppm. It is likely that total Se concentrations are in error because of Se volatilization during sample combustion prior to XRF analyses.

The trace element fractional distributions among the various reservoirs do not show any major trends from soil to soil, or with depth within each soil. Some elements with very low total concentrations exhibit consistently non-uniform behavior. Due to the lower total concentrations of Co, Se, Cu, Pb, and Zn in the control area soil, these elements tend to show less regular behavior in this soil unit when compared to the other two profiles. Aside from this consistent irregularity, which is especially notable in CS1, we believe that most other anomalous behavior can be attributed to being experimental artifacts, and do not speak to usual behavior of these trace elements during sequential extractions from soil samples.

Certain elements may not be completely extracted during the intended step, potentially because the amount in the soil exceeds the amount the extractant is able to withdraw. In other words, the extractant may be the limiting reagent in some cases and does not allow for complete removal of a given element. Other considerations of this extraction procedure include the generalized targeting of each step. Although each step is

intended to pull out a specific fraction, due to the combined effects of the previous consideration as well as the broader effects of chemical weathering that may degrade non-targeted elements, there may be some overlap among reservoirs determined by this method.

For anomalous behavior of elements within certain horizons or extractable fractions, duplicate samples were examined. There were no detectable levels of Co in the CS1 duplicate, but other than this difference, samples were consistent. There were low concentrations of Se in the OM/MO step of CS2, and low concentrations in the WS/EX and AS steps for CS1. CS1 showed no reproducible concentrations in the reducible step for V, but OM/MO levels were roughly the same. In this sample, there also were no RED concentrations of Cr. Cu, Ni, Pb, and Zn showed no great variation between duplicate samples. These few and small inconsistencies between samples indicate that some anomalies observed from the ICP-OES trace element results are not indicative of geochemical trends, but instead represent experimental error or artifact of sampling and analyzing concentrations of elements near detection limits.

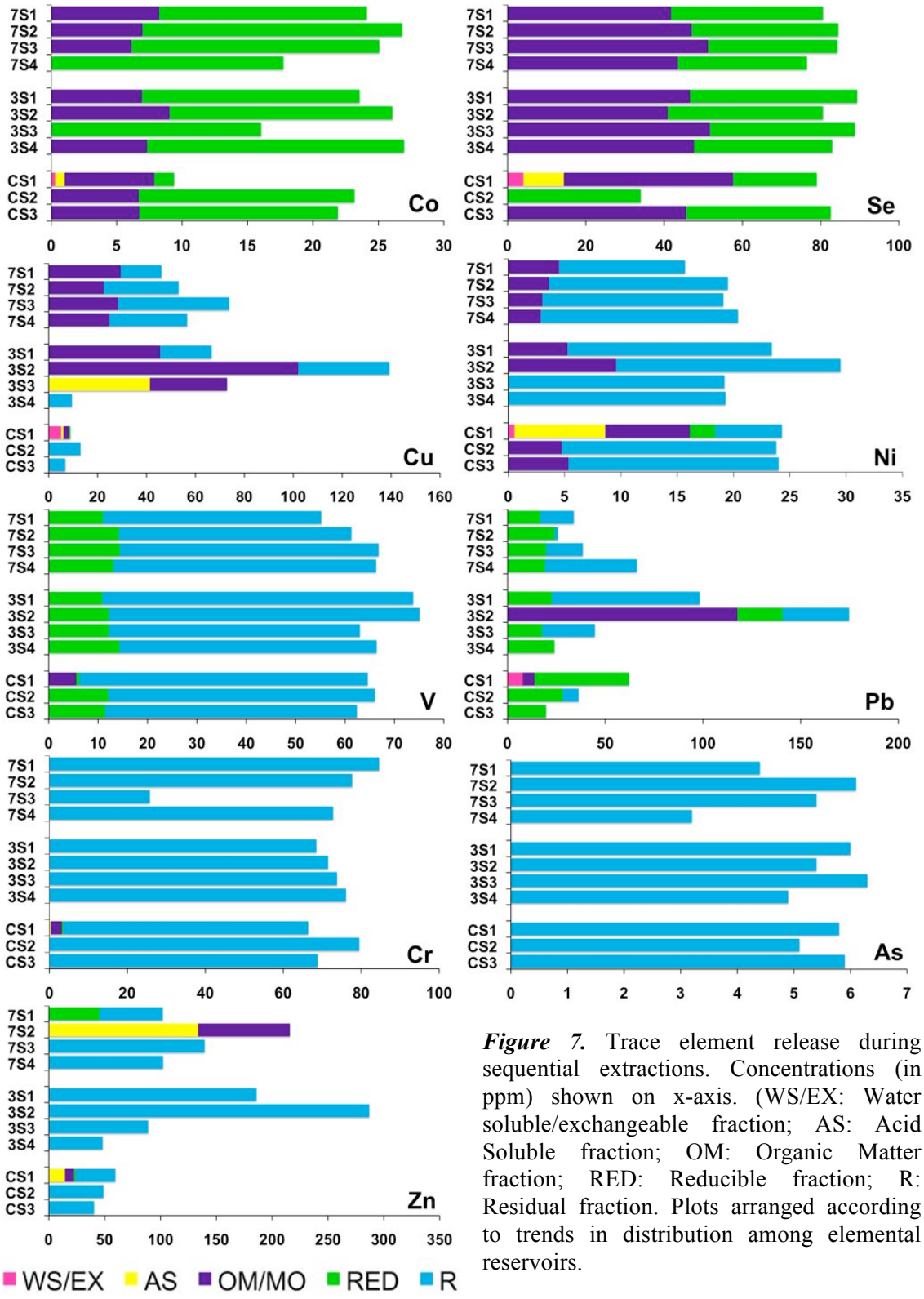

Figure 7. Trace element release during sequential extractions. Concentrations (in ppm) shown on x-axis. (WS/EX: Water soluble/exchangeable fraction; AS: Acid Soluble fraction; OM: Organic Matter fraction; RED: Reducible fraction; R: Residual fraction. Plots arranged according to trends in distribution among elemental reservoirs.

DISCUSSION

Comparison to Other Soil Systems

The trends in heavy metal release observed in this study were generally in agreement with those found in other soil systems. However, not all results were alike, notably in the speciation of Se, V, and Zn. This can be attributed to differences in the order of specific extraction procedures, soil texture and composition, soil pH, and heavy metal speciation (Pauget et al. 2012; Martinez-Vilegas et al. 2004; Janos et al. 2010; Agnieszka et al. 2012).

As determined experimentally in this study, Co is known to be strongly associated with Mn oxides, soil organic matter, and Fe oxides (Bradl 2004; Burns 1976). In one study examining soils from radioactive waste sites, Co was found primarily in the Mn oxide reservoir, with a smaller portion associated with Fe oxyhydroxides (Means et al. 1978). These findings align with the results of this study in the determination of the main reservoirs, although relative concentrations vary. Bangash et al. (1992) suggest that Co adsorption to various surface sites can be reduced by increasing concentrations of Ca and Mg, which could explain this difference.

The extraction of Se for TRC soils differed greatly from the behavior observed by in a prior study of contaminated soils with similar pH and Si, Al, Fe, and Mn concentrations (Lim & Goh 2005). The study by Lim and Goh was able to extract the great majority of Se in the water soluble/exchangeable and strongly adsorbed fractions, which were chemically similar steps to the WS/EX and AS steps in this study. Their results are unlike than those of this study, which determined the clear majority of Se

totals to be extracted from the OM/MO and RED steps; this difference suggests that Se speciation differed between the two studies.

Results from various studies examining the extractability and mobility of Cu were closely aligned with the results of the present investigation, determining large percentages of total Cu to be extractable (Peters 1999). One investigation of soils contaminated by Cu smelting (Grzebisz et al. 1997) found that Cu was mainly extracted in the organic matter step. Another study comparing the mobility of various metals determined Cu to be more mobile than Zn in sandy clay loam soils of moderately acidic pH (Arias et al. 2005). In other soils contaminated with heavy metals from mining, steel factories, and traffic emissions, Cu was determined to be extracted in higher percentages than Ni, Fe, and Cr, similar to the results from TRC. These prior studies are consistent with the present results and other literature describing the behavior of Cu in soils (e.g., Vega et al. 2006).

A sequential extraction study comparing the behavior of Cr and Ni in soils determined that, as at TRC, these elements behave differently (Quantin et al. 2008). These authors found Ni to be much more mobile in soils, and associated with Mn oxides, which is consistent with the substantial percentage of Ni extracted during the OM/MO step. These findings also agree with a third study investigating the mobility of Cr, Ni, and V by means of sequential chemical extractions (Agnieszka & Barbara 2012). In this additional study, Cr was determined to be strongly bound to and incorporated into Fe oxides and primary minerals and was unavailable to plants.

Polednoik & Buhl (2003) found V to be largely non-extractable, but mainly associated with organic matter in the extractable fraction. Agnieszka & Barbara (2012)

determined that V was less mobile than Cr, which differed from the behavior observed in TRC soils. A third sequential extraction study by Zemberyova et al. (2007) also determined V to be dominantly in the residual fraction. The variation in V extractability among these studies is likely due to differences in V speciation.

A study on the sorption behavior of Pb in soil by Martinez-Villegas et al. (2004) experimentally determined that Pb was strongly associated with specific surface sites on Fe oxides, which is consistent with the large fraction of Pb extracted from TRC soils during the RED step, as well as literature previously discussed. Another study by Stipp et al. (2002) examining the role of Fe oxide surfaces as substrates for inorganic contaminants found Pb to be often incorporated into ferrihydrite aggregates. Other studies have found Pb to be strongly associated with humic substances (e.g. Vega et al. 2006; Janos et al. 2010). This is not observed for the majority of TRC soil samples, which could be due to the low organic matter content of these soils.

Studies concerning the extractability of Zn in soil show large variability in the observed speciation. Janos et al. (2010) determined by sequential chemical extractions that Zn was largely immobile in contaminated soils, but a study by Peters (1999) determined that Zn had an extractable fraction exceeding 70%. Maiz et al. (1997) determined that Zn was more mobile and extractable than Mn, Ni, Fe, and Cr in soils contaminated by mining, steel factory operations and traffic emissions. Studies that found Zn to be in non-labile forms agreed that this non-extractable fraction is often found in the phyllosilicate component (Kirpichtchikova et al. 2006; Bradl 2004; Jacquat et al. 2009).

Most studies using chemical extractions to determine the fractionation of As in soils were able to extract this trace element. Findings in the literature generally agreed

that As was strongly associated with Fe oxides that were targeted in the reducible fraction (Novoa-Munoz et al. 2007; Baig et al. 2009; Wenzel et al. 2001). It is likely that the present study was not able to determine speciation of As beyond the portion found in the residual fraction due to total and extracted concentrations near detection limits for both XRF and ICP-OES. Overall, other studies of contaminated soils and the speciation of metals among geochemical pools were in agreement with the extraction results from TRC soils. The results of this study likely differed from the literature due to differences in total concentrations of contaminants, soil pH, and soil composition (Pauget et al. 2012; Martinez-Villegas et al. 2004; Vega et al. 2006; Li et al. 2011).

Environmental Implications

Overall, the data show elevated concentrations of heavy metals in AOC 3 and/or AOC 7 soils when compared with concentrations from the control soil (Table 2). However, the sequential extraction results show that these elevated levels of trace elements, which can be toxic to people, plants, and other biota in high concentrations when released into groundwater, are not easily leached out or released from the various reservoirs (Fig. 7). In spite of indiscriminate waste disposal in the 1940s and 1950s, remediation and natural processes have since immobilized many elements that are considered inorganic contaminants. Co, Se are strongly bound to humic substances or incorporated into Mn-oxides, as shown by their substantial extraction during the OM/MO step; these species are also sequestered in Fe-oxides, as shown by their extraction during the reducible step. Cu and Ni are mostly bound to humic substances or otherwise not labile in soil. V and Pb are adsorbed onto or incorporated into Fe-oxides, or stored in

even less weatherable materials. Cr(III), which is redox-active, and easily oxidizable to Cr(VI) in the presence of Mn-oxides (Fendorf 1995), is not at risk of release, as it is located in a highly recalcitrant phase. As is not found in high levels in these soils, but was determined to be completely immobile. Zn is found in extremely high concentrations in the contaminated AOCs, but found to be in recalcitrant phases.

CONCLUSIONS

The clear majority of the heavy metals at the site, determined in the total element concentrations by XRF, are distributed in non-labile forms and have been successfully immobilized by natural processes and remediation efforts. The elements of concern have been sequestered or non-exchangeably bound to clay surfaces, Fe- and Mn-oxides, and humic substances under moderately acidic soil conditions in alfisols and entisols in a temperate climate. These elements, unless chemically weathered in the presence of harsh solvents or over geologic timescales, pose little to no threat to local water bodies or potable water sources. Further studies using spectroscopic techniques in combination with extraction procedures, such as those used in this study, would be able to provide additional information on the nature of elemental speciation in association with these immobilizing materials.

REFERENCES

Agnieszka, J. and Barbara, G. (2012) Chromium, nickel and vanadium mobility in soils derived from fluvioglacial sands. *Journal of Hazardous Materials,* 237-238, 315-322.

Anju, M. & Banerjee, D.K. (2009). Associations of cadmium, zinc, and lead in soils from a lead and zinc mining area as studies by single and sequential extractions. *Environmental Monitoring and Assessment*, 176, 67-85.

Arias, M., Perez-Novo, C., Osorio, F, Lopez, E., and Soto, B. (2005) Adsorption and desorption of copper and zinc in the surface layer of acid soils. *Journal of Colloid and Interface Science*, 288, 21-29.

Baid, J. A., Kazi, T.G., Arain, M.B., Shah, A.Q., Sarfraz, R. A., Afridi, H.I., Kandhro, G.A., Jamali, M.K., and Khan, S. (2009) Arsenic fractionation in sediments of different origins using BCR sequential and single extraction methods.

Ball, L. B., Kress, W.H., Anderson, E.D., Teeple, A.P., Ferguson, J.W., and Colbert, C.R. (2004) Surface Geophysical Investigation of the Areal and Vertical Extent of Metallic Waste at the Former Tyson Valley Powder Farm Near Eureka, Missouri, Spring 2004. US Geological Survey, Reston, Virginia

Bangash, M.A., Harif, J., and Ali Khan, M. (1992) Sorption behavior of cobalt on illitic soil. *Waste Management*, 12, 29-38.

Beesley, L., Moreno-Jimenez, E., Clemente, R., Lepp, N., and Dickinson, N. (2010). Mobility of arsenic, cadmium and zinc in a multi-element contaminated soil profile assessed by *in-situ* soil pore water sampling, column leaching and sequential extraction. *Environmental Pollution*, 158, 155-160.

Benjamin, M.M. and Leckie, J.O. (1981) Multiple-site adsorption of Cd, Cu, Zn, and Pb on Amorphous Iron Oxyhydroxide. *Journal of Colloid and Interface Science*, 79, 209-221.

Bradl, H.B. (2004) Adsorption of heavy metal ions on soils and soils constituents. *Journal of Colloid and Interface Science*, 277, 1-18.

Brantley S. L., Kubicki J. D., and White A. F. (2008) Kinetics of Water-Rock Interaction, pp. 833. Springer.

Burns, R.G. (1976) The uptake of cobalt into ferromanganese nodules, soils, and synthetic manganese (IV) oxides. *Geochimica et Cosmochimica Acta*, 40, 95-102.

Burt, R., Weber, T., Park, S., Yochum, S., and Ferguson, R. (2011). Trace element concentration and speciation in selected mining-contaminated soils and water in Willow Creek Floodplain, Colorado. *Applied and Environmental Soil Science*, 2011, 20 p.

Burt, R., Wilson, M.A., Keck, T.J., Dougherty, B.D., Strom, D.E., and Lindahl, J.A. (2003). Trace element speciation in selected smelter-contaminated soils in Anaconda and Deer Lodge Valley, Montana, USA. *Advances in Environmental Research*, 8, 51-67.

Cornell, R.M. & Schwertmann, U. (2003) The Iron Oxides: Structure, Properties, Reactions, Occurrences and Uses. WILEY-VCH Verlag GmbH & Co. 664 p.

Couture, R. A.; Dymek, R. F., A reexamination of absorption and enhancement effects in X-ray fluorescence trace element analysis. *Am. Mineral.* 1996, *81*, 639-650.

Couture, R. A.; Smith, M. S.; Dymek, R. F., X-ray fluorescence analysis of silicate rocks using fused glass discs and a side-window Rh source tube: Accuracy, precision and reproducibility. *Chem. Geol.* 1993, *110*, 315-328.

Dong, E., Nelson, Y.M., Lion, L.W., Shuler, M.L., and Ghiorse, W.C. (2000) Adsorption of Pb and Cd onto metal oxides and organic material in natural surface coatings as determined by selective extractions: new evidence for the importance of Mn and Fe oxides. *Water Resources*, 34, 427-436.

Favas, P.J.C., Pratas, J., Gomes, M.E.P., and Cala, V. (2011). Selective chemical extraction of heavy metals in tailings and soils contaminated by mining activity: Environmental Implications. *Journal of Geochemical Exploration*, 111, 160-171.

Fendorf, S.E. (1995) Surface reactions of chromium in soils and waters. *Geoderma*, 67, 55-71.

Grzebisz, W., Kocialkowski, W.Z., and Chudzinski, B. (1997) Copper geochemistry and availability in cultivated soils contaminated by a copper smelter. *Journal of Geochemical Exploration*, 58, 301-307

Hartley, W. & Lepp, N.W. (2008) Remediation of arsenic contaminated soil by iron-oxide application, evaluated in terms of plant productivity, arsenic and phytotoxic metal uptake. *Science of the Total Environment*, 390, 35-44.

Jacquat, O., Voegelin, A, Juillot, F., and Kretzschmar, R. (2009) Changes in Zn speciation during soil formation from Zn-rich limestones. *Geochimica et Cosmochimica Acta*, 71, 5554-5571.

Jacquat, O., Voegelin, A., and Kretzschmar, R. (2009) Soil properties controlling Zn speciation and fractionation in contaminated soils. *Geochimica et Cosmochimica Acta,* 73, 5256-5272.

Janos, P., Vavrova, J., Herzogova, J., and Pilarova, V. (2010) Effects of inorganic and organic amendments on the mobility (leachability) of heavy metals in contaminated soil: A sequential extraction study. *Geoderma*, 159, 335-341.

Li, B., Zhang, H., Ma, Y., and McLaughlin, M.J. (2011) Influences of soil properties and leaching on nickel toxicity to barley root elongation. *Ecotoxicology and Environmental Safety*, 74, 459-466.

Lim, T.-T., and Goh, K.-H. (2005) Selenium extractability from a contaminated fine soil fraction: implication on soil cleanup. *Chemosphere*, 58-91-101.

Maiz, I., Arambarri, I., Garcia, R., and Millan, E. (2000) Evaluation of heavy metal availability in polluted soils by two sequential extraction procedures using factor analysis. *Environmental Pollution*, 110, 3-9.

Maiz, I., Esnaola, M.V., and Millan, E. (1997) Evaluation of heavy metal availability in contaminated soils by a short sequential extraction procedure. *The Sciences of the Total Environment,* 206, 107-115.

Means, J.L., Crerar, D.A., and Borcsik, M.P. (1978) Adsorption of Co and selected actinides by Mn and Fe oxides in soils and sediments. *Geochimica et Cosmochimica Acta*, 42, 1763-1773.

Mikutta, R., Kleber, M., Kaiser, K., and Jahn, R. (2005) Review: Organic Matter Removal from Soils using Hydrogen Peroxide, Sodium Hypochlorite, and Disodium Peroxodisulfate. *Soil Science Society of America Journal*, 69, 120-135.

Novoa-Munoz, J.C., Queijeiro, J.M.G., Blanco-Ward, D., Alvarez-Olleros, C., Garcia-Projeja, E., and Martinez-Cortizas, A. (2007) Arsenic fractionation in agricultural acid soils from NW Spain using a sequential extraction procedure. *Science of the total Environment*, 378, 18-22.

Pauget, B., Gimbert, F., Scheifler, R., Coeurdassier, M. and deVaufleury, A. (2012) Soil parameters are key factos to presict metal bioavailability to snails based on chemical extractant data. *Science of the Total Environment*, 431, 413-425.

Pelfrene, A., Waterlot, C., Mazzuca, M., Nisse, C., Bidar, G., and Douay, F. (2011). Assessing Cd, Pb, Zn human bioaccessibility in smelter-contaminated agricultural topsoils (northern France). *Environmental Geochemistry and Health*, 33, 477-493.

Pendias, H., and Kabata-Pendias, A. (2000) Trace Elements in Soils and Plants, 3rd ed. CRC Press.

Peters, R.W. (1999) Chelant extraction of heavy metals from contaminated soils. *Journal of Hazardous Materials*, 66, 151-210.

Poledniok, J., and Buhl, F. (2003) Speciation of vanadium in soil. *Talanta*, 59, 1-8.

Quantin, C., Ettler, V., Garnier, J., and Sebek, O. (2008) Sources and extractability of chromium and nickel in soil profiles developed on Czech serpentinites. *C.R. Geoscience*, 340, 872-882.

Rai, D.; Hess, N. J.; Rao, L. F.; Zhang, Z. C.; Felmy, A. R.; Moore, D. A.; Clark, S. B.; Lumetta, G. J., Thermodynamic model for the solubility of $Cr(OH)_3(am)$ in concentrated NaOH and NaOH-$NaNO_3$ solutions. *J. Solut. Chem.* 2002, *31*, 343-367.

Rai, D.; Moore, D. A.; Hess, N. J.; Rao, L.; Clark, S. B., Chromium(III) hydroxide solubility in the aqueous Na^+-OH^--$H_2PO_4^-$-HPO_4^{2-}-PO_4^{3-}-H_2O system: A thermodynamic model. *J. Solut. Chem.* 2004, *33*, 1213-1242.

Schwertmann, U., and Pfab, G. (1996) Structural vanadium and chromium in lateritic iron oxides: Genetic implications. *Geochimica et Cosmochimica Acta*, 60, 4279-4283.

Seby, F., Potin Gautier, M., Lespes, G. and Astruc, M. (1997) Selenium speciation in soils after alkaline extraction. *The Science of the Total Environment*, 207, 81-90.

Stipp, S.L.S., Hansen, M., Kristensen, R., Hochella, M.F., Bennedsen, L., Dideriksen, K., Balic-Zunic, T., Leonard, D., and Mathieu, H.-J. (2002) Behavior of Fe-oxides relevant to contaminant uptake in the Environment. *Chemical Geology*, 190, 321-337.

Tariq, S.R. & Bashir, A. (2012) Speciative distribution and bioavailability of metals in agricultural soils receiving industrial wastewater. *Environmental Monitoring and Assessment*, 184, 4609-4622.

Shang and Zelazny (2008) *Methods of Soil Analysis, Part 5. Mineralogical Methods.* Selective Dissolution Techniques for Mineral Analysis of Soils and Sediments.

Vega, F.A., Covelo, E.F., and Andrade, M.L. (2006) Competitive sorption and desorption of heavy metals in mine soils: Influence of mine soil characteristics. *Journal of Colloid and Interface Science*, 298, 582-592.

Violante, A., Arienzo, M., Sannino, F., Colombo, C., Piccolo, A., and Gianfreda, L. (1999) Formation and characterization of OH-Al-humate-montmorillonite complexes. *Organic Geochemistry*, 30, 461-468.

Wenzel, W.W., Kirchbaumer, N., Prohaska, T., Stingeder, G., Lombi, E., and Adriano, D.C. (2001) Arsenic fractionation in soils using an improved sequential extraction procedure. *Analytica Chimica Acta*, 436, 309-323.

Yin, Y., Impellitteri, C.A., You, S., and Allen, H.E. (2002) The importance of organic matter distribution and extract soil: solution ratio on the desorption of heavy metals from soils. *The Science of the Total Environment*, 287, 107-119.

Yusuf, K.A. (2007). Sequential Extraction of Lead, Copper, Cadmium and Zinc in soils near Ojota Waste Site. *Journal of Agronomy*, 6, 331-337.

Zemberyova, M., Jankovic, R., Hagarova, I., and Kuss, H.-M. (2007). Electrothermal atomic absorption spectrometric determination of vanadium in extracts of soil and sewage sludge certified reference materials after fractionation by means of the Communities Bureau of Reference modified sequential extraction procedure. *Spectrochimica Acta Part B*, 62, 509-513.